J Fluoresc (2015) 25:1117–1126
DOI 10.1007/s10895-015-1602-5

ORIGINAL ARTICLE

Red Emitting Coumarins: Insights of Photophysical Properties with DFT Methods

Abhinav B. Tathe[1] · **Lydia Rhyman**[2] · **Ponnadurai Ramasami**[2,3] · **Nagaiyan Sekar**[1]

Received: 7 April 2015 / Accepted: 15 June 2015 / Published online: 3 July 2015

Abstract Red emitting dyes are of interest in various technological applications. Coumarins, though being an important class of fluorescent molecules, those with red emission, have been rarely studied theoretically. The structural and electronic aspects of three novel red emitting coumarins were studied using DFT and TD-DFT methods. The functionals employed were the hybrid functionals B3LYP, CAM-B3LYP, PBE0 and the highly parameterized empirical functional M06. The geometry at ground state reveals the electron donor N,N-diethylamino group is coplanar with the chromophoric system and the nitrile group induces a red shift to the absorption and emission. The electronic energies and dipole moments were solvent dependent. The basis sets and functionals were benchmarked for their performance with these molecules. B3LYP has been proved to be more efficient in computations whereas the basis sets do not have noticeable effect on the electronic properties. However, adding a polarization function to the basis set has improved the calculation of vertical excitation. The B3LYP functional gives maximum absolute deviation of 0.20 eV in calculating the vertical excitations and 0.18 eV for emission.

Keywords Coumarins · DFT · TD-DFT · Vertical excitation

Electronic supplementary material The online version of this article (doi:10.1007/s10895-015-1602-5) contains supplementary material, which is available to authorized users.

✉ Nagaiyan Sekar
n.sekar@ictmumbai.edu.in; nethi.sekar@gmail.com

Ponnadurai Ramasami
ramchemi@intnet.mu

[1] Tinctorial Chemistry Group, Department of Dyestuff Technology, Institute of Chemical Technology, N. P. Marg, Matunga, Mumbai, MH 400019, India

[2] Computational Chemistry Group, Department of Chemistry, Faculty of Science, University of Mauritius, Réduit 80837, Mauritius

[3] Department of Pharmaceutical Chemistry, Faculty of Pharmacy, King Saud University, P.O. Box 2457, Riyadh 11451, Saudi Arabia

Introduction

The red emitting dyes are of interest in the area of OLED [1–4], protein tracking [5], multicolor imaging [6], far-field optical nanoscopy [7, 8]. The red emitting dyes are important in OLEDs to complement their blue [9, 10] and green [11, 12] dye counterparts in fabrication of displays. In biological applications, red emitting dyes stand high and apart due to their ability to produce emission signals discrete from the autofluorescence [13–15] of biomolecules (195–600 nm), low energy excitation and emission in biological window [16, 17]. The optics used for the red region is simpler, as the scattering effect for the red region is minimal and the sources such as dye lasers in the red region are readily available [18]. In this way, the red emitting probes provide the bio-analyst with a less noisy, higher penetrating and simpler technique to study the various biological phenomena.

There are various classes of dyes available for the purpose of emission in red region, such as cyanines [19–23], xanthenes [24–27], BODIPY [28–30], dicyanovinyls [31–33]. Design and synthesis of red emitting dyes are gaining interest in recent years [34–38]. The molecules of coumarin class are known to be highly fluorescent [39] with moderate to good quantum yields [40] and are used in biological applications such as fluorescent markers for proteins [41], cellular imaging [42] and lasers [43]. Coumarin dyes are known to have blue to green fluorescence and there are successful attempts reported in the literature to shift the excitation and emission wavelength

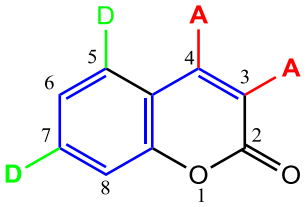

Fig. 1 Positions of donors and acceptors on a coumarin core important for red absorption/emission

of coumarin dyes towards red region [44, 45]. For the red absorption/emission in coumarin core, the positions of donors and acceptors are very important and are illustrated in Fig. 1. The positions 5 and 7 when substituted with a donor moiety such as –OH, $-NEt_2$, $-NH_2$ and $-OCH_3$ and the positions 3 and 4 substituted with acceptors like –CN, −COOEt and benzazolyl group, the coumarin fluorophore experiences a red shifted absorption and hence red shifted emission. Increasing the rigidity of the donor [46] and acceptor [47] groups also adds to the red shift of the coumarin molecules. The substitution at 4-position by –CN group (an acceptor) induces a red shift in the emission of coumarins [44]. Investigations in red absorbing and red emitting coumarins constitute a fertile area of industrial research [48–52].

The donor-acceptor relationships pertaining to the photophysical behavior of the coumarin molecules can be well understood using the quantum chemical computations. A significant work in understanding the structural and photophysical properties was done by Cave et al. [53]. The Pople's split valence triple zeta basis sets with added polarization function 6-311G(d,p) was employed in conjunction with the popular hybrid B3LYP (Becke3-Lee-Yang-Parr hybrid functional), MPW1PW91(Perdew-Wang exchange as modified by Adamo and Barone combined with PW91 correlation) and PBE0 functionals to estimate the dipole moments at ground and excited states for coumarin 151 and 120. The results were compared with the ZINDO, CIS, CASSCF and CASPT2 methods. The system water-coumarin 151 complex was also studied with above methods and found to be in good

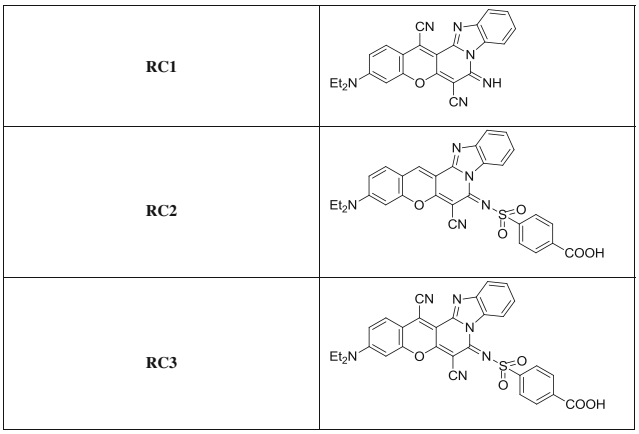

Fig. 2 Red emitting coumarins

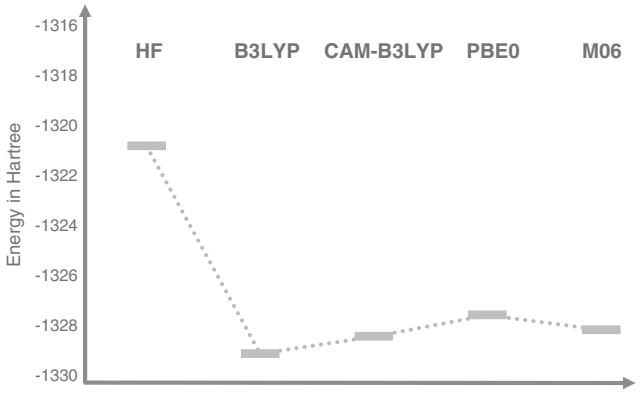

Fig. 3 Energy computed using 6-311++G(2d,p) basis set and various functionals and HF method for **RC1** in CH_3CN

agreement with the experimental results. UV-visible spectrum and IR in solution phase was estimated for coumarin molecules with the SCRF (Self-Consistent Reaction Field) formalism [54]. The time-dependent density functional theory (TD-DFT) calculations with the hybrid functionals BLYP, B3LYP, MPW1PW91, PBE and PBE0 were worked out by Cave et al. [55]. The basis sets used were the split valence 6-31G(d), 6-31+G(d), 6-311G(d,p) and 6-311+G(d,p) and no significant difference was found in the properties such as excitation energies. The Polarizable Continuum Model (PCM) developed by Tomasi et al. [56] and Onsager Polarizable Point Dipole Model [57] was used to study the solvation effects of these molecules.

Table 1 Solvent stabilization energies (kcal/mol) of **RC1**, **RC2** and **RC3** in various solvents calculated with HF and various functionals and 6-311++G(2d,p) basis set

RC1				
	CH_3CN	$CHCl_3$	DMSO	Gas
HF	17.3	12.9	17.5	0.0
B3LYP	16.5	11.7	16.7	0.0
CAM-B3LYP	16.3	11.6	16.5	0.0
PBE0	16.3	11.5	16.5	0.0
M06	16.2	11.5	16.4	0.0
RC2				
HF	28.5	Not Available	28.9	0.0
B3LYP	25.1		25.4	0.0
CAM-B3LYP	25.4		25.8	0.0
PBE0	24.9		25.2	0.0
M06	21.9		22.6	0.0
RC3				
HF	29.2	Not Available	29.6	0.0
B3LYP	26.6		26.9	0.0
CAM-B3LYP	26.5		26.9	0.0
PBE0	25.9		26.3	0.0
M06	25.6		26.0	0.0

All the values expressed in kcal/mol

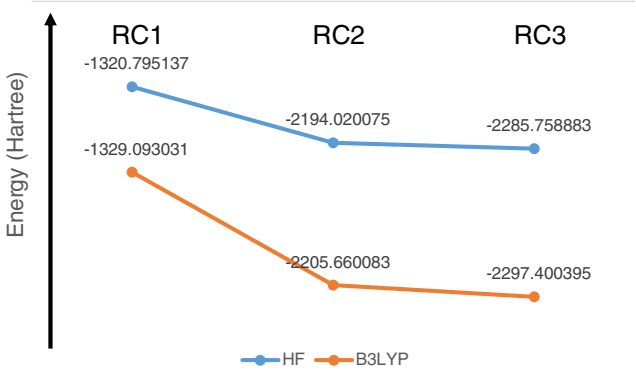

Fig. 4 Energy (in Hartree) of **RC1**, **RC2** and **RC3** in CH_3CN using HF/6-311++G(2d,p) and B3LYP/6-311++G(2d,p) methods

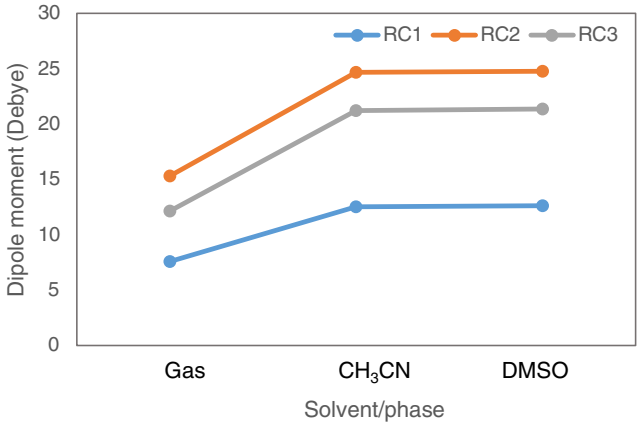

Fig. 6 Dipole moments in Debye for **RC1**, **RC2** and **RC3** in various solvents at B3LYP/6-311++G(2d,p) level

An a priori approach of assessing the desired photophysical properties prior to synthesis can save a lot of efforts and minimize the use of environmentally hazardous chemicals. The computational methods are to be standardized and tried before they can be used for such applications. This can make predictions closer to the observed photophysical properties. Towards this end, in this paper a complete focus has been laid to rationalise the practical observations with the help of ab initio methods. There are many such reports investigating the photophysics of the coumarins with the help of DFT [58–64]. The coumarin molecules taken up for the studies were relatively smaller (30–40 atoms). To have a better method to predict the photophysical properties of real world functional molecules, there is a need to work on the analogous molecules.

The molecules studied (Fig. 2) were synthesized by Huang and co-workers and their photo-physical properties in various solvents are known [45]. The molecules were reported to show the excitation and emissions in the range of 570–721 nm and they are sensitive to the solvent environment. These molecules represent a class of red emitting coumarins with a rigidized acceptor moiety. The study of the properties of these molecules can reinforce the base of computational studies of more complicated red emitting coumarins falling in this class.

In this paper, we have attempted to give a theoretical explanation to the photophysical behaviour of the above dyes in solvent environment using DFT calculations. The observed substituent effect as well as solvent effect on absorption wavelength were correlated with the theoretical calculations. This will help in understanding the suitability of the computational methods to interpret the photophysical properties of the red emitting coumarins.

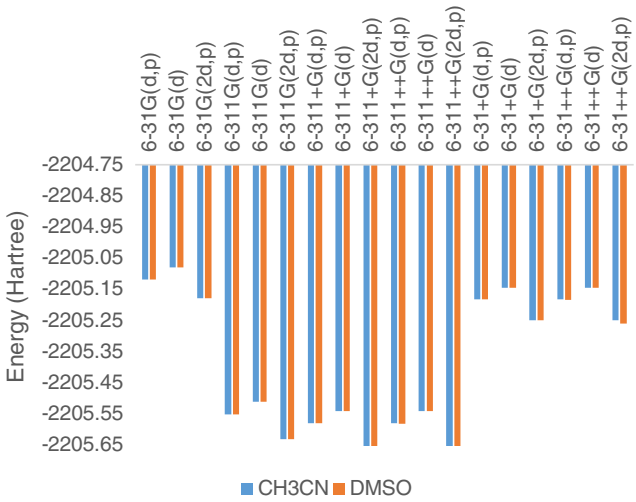

Fig. 5 Energies (Hartree) calculated for **RC2** using B3LYP functional and various basis set

Methods/Computational Strategy

DFT method [65] for the ground state optimisations and TD-DFT [66] for the vertical excitation computations were used. The functionals used were B3LYP (Becke3-Lee-Yang-Parr hybrid functional) [67, 68], CAM-B3LYP [69], PBE0 [70] which are hybrid functionals. The highly parameterized empirical M0X series which account for the non-covalent interactions as well as "medium range" electron correlation, M06 [71] was also used. The use of M06 in computations to study

Table 2 Angle of pyramidalization in DMSO for **RC1**, **RC2** and **RC3** in HF and various functionals and 6-311++G(2d,p)

	RC1	RC2	RC3
HF	0.3	0.3	0.2
B3LYP	0.8	0.3	0.2
CAM-B3LYP	1.9	0.1	0.2
PBE0	2.03	0.0	0.2
M06	2.0	0.2	0.2

Angles in °

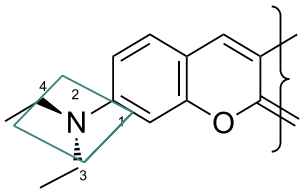

Fig. 7 Angle (Degree) of pyramidalization

the photophysical properties of coumarin is not documented in the literature. The results of the HF method were also compared with the DFT functionals. The solvents considered were chloroform ($CHCl_3$), dimethyl sulfoxide (DMSO) and acetonitrile (CH_3CN). The solvation model employed was PCM (Polarizable Continuum Model) [56]. The various Pople's basis sets [72, 73] like 6-31G(d), 6-311G(d), 6-31+G(d), 6-311+G(d), 6-31++G(d), 6-311++G(d), 6-31G(d,p), 6-311G(d,p), 6-31+G(d,p), 6-311+G(d,p), 6-31++G(d,p), 6-311++G(d,p), 6-31G(2d,p), 6-311G(2d,p), 6-31+G(2d,p), 6-311+G(2d,p), 6-31++G(2d,p) and 6-311++G(2d,p) were used. The optimized structures were confirmed to be the local minima on potential energy surface by vibrational analysis and they show no imaginary frequencies. The emission energies were calculated using relaxed excited state geometry. All the computations were performed using the Gaussian 09 package [74] running on GridChem [75, 76].

Result and Discussion

The geometry at the ground and excited states plays an important role in the photophysical behaviour of the organic molecules. The geometry optimization was performed using different functionals and basis sets and the energies of the molecules were estimated. The effect of the functionals on the estimated energies of the molecule were studied and are presented in Fig. 3 (Additional data provided in the Electronic supplementary material). The hybrid functionals B3LYP and

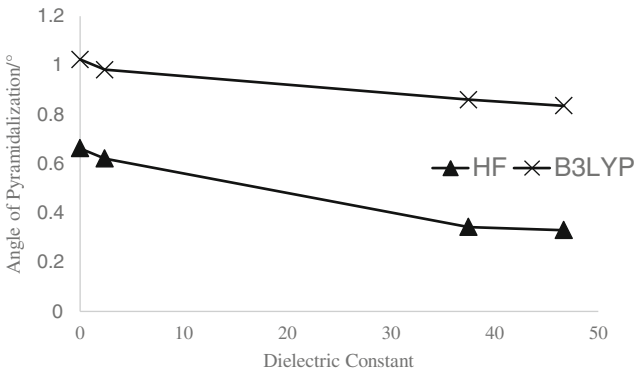

Fig. 8 Dielectric constant dependent angle of pyramidalization calculated for **RC1**

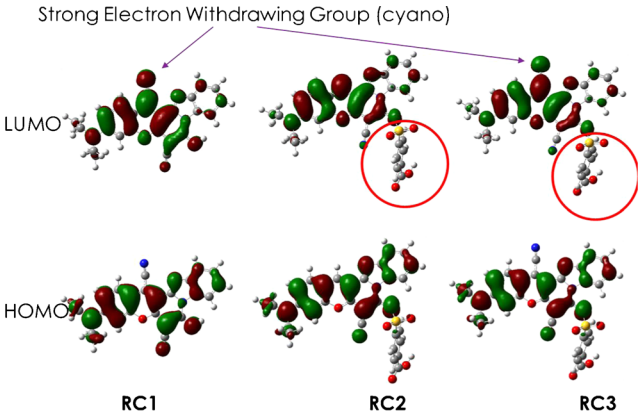

Fig. 9 FMO diagram for compound **RC1**, **RC2** and **RC3** in DMSO

CAM-B3LYP compute the lower energies, compared to other functionals. The M06 functional computes energy closer to CAM-B3LYP and lower than PBE0. The HF calculates higher electronic energy of the molecules.

The energy of the molecules also depends on the solvents used and has different stabilization energy in different solvents (SI Table 7). The solvent environment stabilizes the molecular geometry. The extent of the stabilization depends on the polarity of solvent. The gas phase molecular energy was taken as reference and the solvent stabilization energies were calculated (Table 1). The stabilization energies using HF level of theory were calculated to be larger compared to the other methods, whereas the calculated values from the other functionals are close (~0.2–0.6 kcal/mol) to each other (Fig. 4).

The effect of basis set on calculating molecular energies was studied with various basis sets. The improvement in the molecular energy was monitored as a function of change in basis set. The variation in basis sets were made based on the double zeta, triple zeta basis sets with polarization and diffused functions. Various combinations available in the Pople's basis set were applied. There was a variation found based on the nature of the basis sets. The improvement in the calculation is achieved by mixing the triple zeta basis set with polarization on heavy atoms and diffused functions. The triple zeta 6-311G basis set predicted lower values of energy than

Table 3 Absorption and emission of compound **RC1, RC2** and **RC3** in various solvents*

	DMSO		CH3CN		CHCl3	
	λabs	λems	λabs	λems	λabs	λems
RC1	640	689	630	677	631	660
RC2	570	607	565	603	–	–
RC3	673	715	663	704	–	–

All the values expressed in nm

*Data from the literature [45]

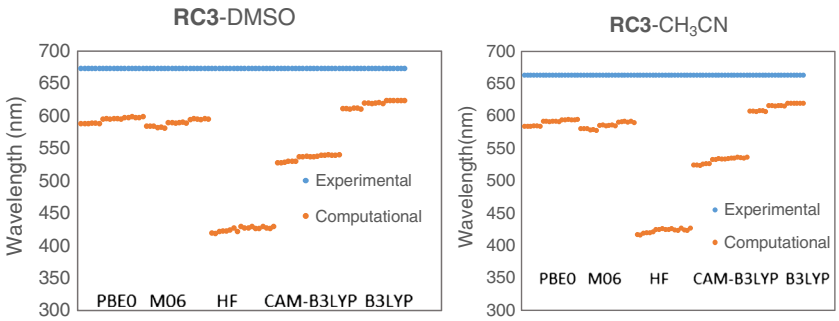

Fig. 10 Effect of functionals/ methods on the computation of vertical excitations of **RC3**

the 6-31G basis set. The performance of the basis set is given as a representative example with **RC2** using the B3LYP functional. Though the DFT method is known to be less basis set dependent, here in case of these molecules the triple zeta basis set computed lower energies. Further addition of polarization and diffused functions does not have a linear effect on the energy values (Additional data is provided in Electronic supplementary material) (Fig. 5).

Dipole Moments

The trends in dipole moments calculated for the molecules are shown in Fig. 6. The trend shows that the dipole moments are solvent dependent and it is the highest for **RC2** molecule where–CN group is not found at 4 position. In case of **RC3** the –CN group has compensated for the dipole moment change occurred due to addition of a polar sulphonyl benzoic acid. The dipole moment of **RC1** remains in the range of 7.58 D to 12.60 D due to the lack of sulphonyl benzoic acid group. The dipole moments for the molecules **RC2** and **RC3** are in the range of 12.13 D to 24.77D in the solvents.

Ground State Geometry

The strength as well as positioning of the donor and acceptor groups contribute to the various properties of the chromo/ fluorophores. We optimized the structures with the help of the analytic gradient available at the ground state of the molecule. The diethylamino group is a common donor for all the three molecules and calculations reveal that the strength of the group varies depending upon the solvents. This has translated to the angle of pyramidalization. Pyramidalization is accompanied by the deviation from planarity of the three atoms attached to nitrogen (180-φ C1-N2-C3-C4). Smaller the value, more the donor is in-plane and available for the interaction with the chromophoric system. The angle of pyramidalization has decreased from non-polar to polar solvents and this implies that the planarity and consequently the donor strength of diethylamino group increases. The different functionals and the angles of pyramidalization are given in Table 2. The HF/6-311++G(2d,p) method shows lowest pyramidalization angles, but there is no clear trend among the functionals. All the values indicate that good planarity is achieved in polar solvents as compared to non-polar solvents. Among **RC1, RC2** and **RC3**, the molecule **RC1** shows highest deviation from planarity in the donor group (Figs. 7 and 8).

The acceptor is benzimidazole unit and it is in-plane with the coumarin chromophoric system which is a common observation for all the three molecules. The other acceptor is cyano (−CN) and remains in the same plane due to linear geometry around carbon atom of cyano group and aromatic (sp^2 hybrid) carbon atom of coumarin.

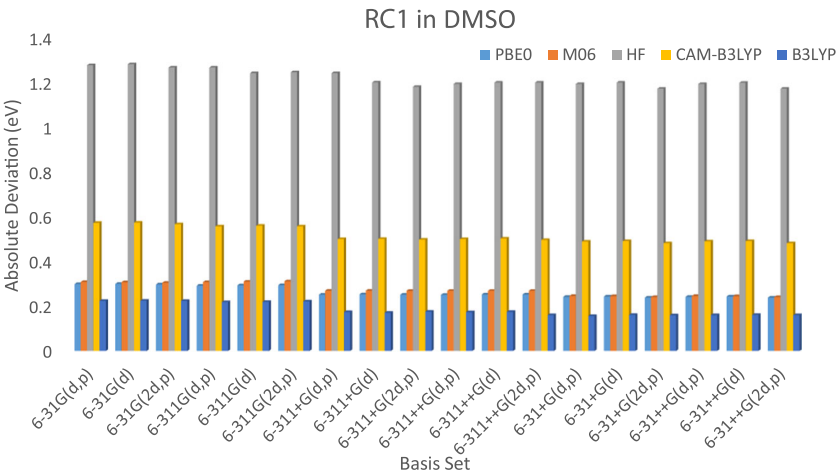

Fig. 11 Absolute deviation using various functional/method and basis sets in computing the vertical excitations for **RC1** in DMSO

The frontier molecular orbital diagram of the molecules **RC1**, **RC2** and **RC3** indicates that –CN group at 4-position has a great impact on the absorption and emission properties of the molecule. The electron density on –CN group at LUMO level is clearly seen. Molecule **RC1**, though does not have sulphonamide group which is an acceptor, absorbs at a longer wavelength than the molecule **RC2**. The sulphonyl benzoic acid group does not remain in-plane with the chromophoric system and thus does not contribute towards the LUMO molecular orbital (see Fig. 9).

Vertical Excitations

The experimental data for vertical excitations of **RC1**, **RC2** and **RC3** is tabulated in the Table 3. There is a positive solvatochromism exhibited by these molecules. The same solvatochromic behaviour is predicted by all the computational methods. The oscillator strengths and orbital contributions were also estimated. Interestingly in all the compounds, the contributing transition for the absorption is HOMO→LUMO (**RC1**: 106→107, **RC2**: 147 →148, **RC3**: 153→154). The oscillator strengths were also calculated and found to be dependent on the functional and are less sensitive to the basis set used (See Electronic supplementary material).

The vertical excitations for **RC1**, **RC2** and **RC3** were calculated with the various basis sets and functionals to assess their utility. There is a clear trend in calculating the vertical excitations among the functionals. The order of the variation is HF > CAM-B3LYP > M06 > PBE0 > B3LYP, where HF has deviated most from the experimental values. Though the B3LYP and PBE0 functionals perform better, CAM-B3LYP which is a hybrid functional is found to be less appropriate. M06 functional, on the other hand, perform better than the HF and CAM-B3LYP (Fig. 10).

To understand the overall trend in the performance of the functionals in computing the vertical excitations energies of the molecules the data was statistically analysed. Figure 11 shows the performance of the various functionals and HF method and basis sets in calculating the vertical excitations of compound **RC1** in DMSO in terms of absolute deviation.

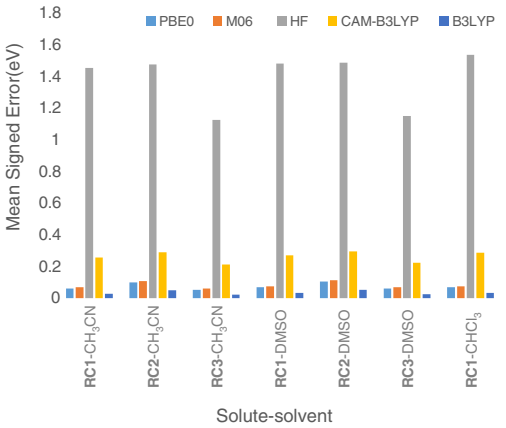

Fig. 12 Mean signed error in computation of the vertical excitations with HF method and various functionals

The B3LYP functional performs best with an absolute deviation of less than 0.2 eV. The vertical excitation value computed with HF method deviates by more than 1.2 eV, whereas the PBE0 and M06 functionals shown deviation of 0.3 eV from the experimental value (Table 4).

The mean absolute error ranges from 0.15 to 1.24 eV. The mean absolute deviation (MAD) values vary with the solvent used. The MAD for acetonitrile is lower than the DMSO consistently using all the functionals and this may be due to the limitation of PCM (Polarizable Continuum Model) to define the solvent environment of DMSO as compared to the acetonitrile solvent. B3LYP functional has shown the least values of MAD and qualifies as the best among the other functionals studied.

The mean signed difference (MSD) or mean signed error (MSE), is a sample statistic that summarises the accuracy of the predicted value with a value to be estimated. It is one of a number of statistics that can be used to assess an estimation procedure. Here the MSE for B3LYP, M06 and PBE0 remains well below 0.12 eV. Only exceptions are for CAM-B3LYP and HF methods. Out of which CAM-B3LYP gives the highest MSE below 0.30 eV and HF method gives a value of 1.13 to 1.54 eV (see Fig. 12).

Table 4 Mean absolute deviation in HF and various functional (in eV)

	PBE0	M06	HF	CAM-B3LYP	B3LYP
RC1-CH_3CN	0.25	0.26	1.21	0.51	0.17
RC2-CH_3CN	0.32	0.33	1.22	0.54	0.23
RC3-CH_3CN	0.23	0.25	1.06	0.46	0.15
RC1-DMSO	0.26	0.28	1.22	0.52	0.19
RC2-DMSO	0.33	0.34	1.22	0.55	0.23
RC3-DMSO	0.25	0.26	1.07	0.47	0.16
RC1-$CHCl_3$	0.27	0.28	1.24	0.54	0.19

Table 5 Root mean squared (RMS) error in computing vertical excitations with HF method and different functionals (in eV)

	PBE0	M06	HF	CAM-B3LYP	B3LYP
RC1-CH_3CN	0.25	0.26	1.21	0.51	0.17
RC2-CH_3CN	0.32	0.33	1.22	0.54	0.23
RC3-CH_3CN	0.23	0.25	1.06	0.46	0.15
RC1-DMSO	0.27	0.28	1.22	0.52	0.19
RC2-DMSO	0.33	0.34	1.22	0.55	0.23
RC3-DMSO	0.25	0.26	1.07	0.48	0.17
RC1-$CHCl_3$	0.27	0.28	1.24	0.54	0.19

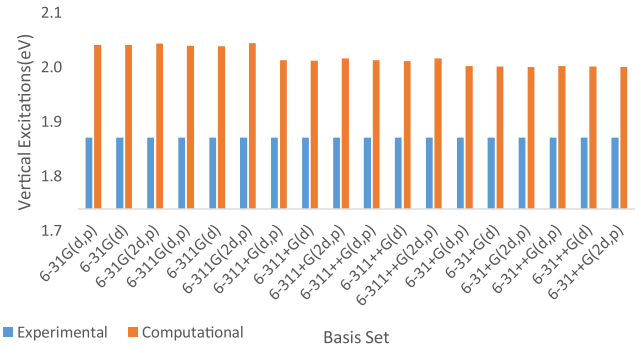

Fig. 13 Effect of basis sets on vertical excitation computations using B3LYP functional for **RC1** in CH_3CN

Root mean squared error (RMS) is the difference between the values predicted by a model and the values actually observed. The RMS error represents the sample standard deviation of the differences between the predicted values and the observed values. In this case, the deviation for B3LYP functional was found to be the lowest and the highest for HF method. The HF method predicts the vertical excitations with a very large difference, 8 to 10 times more than the B3LYP functional (Table 5).

Effect of Basis Set on Vertical Excitation

The vertical excitation energies have been computed to be higher than the experimentally observed values by all the functionals and basis sets. The different basis sets studied has shown that there is only factor which has added to the computation having closer vertical excitation value i.e., addition of polarization function to the basis set. However, no improvement is observed when polarization is extended to the lighter atoms during computations i.e., to the H atom in molecule. The computation of vertical excitation was not improved by the addition of diffused functions as well as extending the basis sets from double zeta to triple zeta type of basis sets (Fig. 13).

Emission Computations

The emission energies were calculated taking the relaxed excited state geometry, and calculating the ground state vertical excitation energy for that structure. From the calculations of the vertical excitation, it is understood that the basis set has a little effect on the accuracy of results. The vertical excitation energies are more functional dependent and do not depend on the basis sets. Considering these, the emission energies were calculated at the minimal basis set i.e., 6-31G(d), which also saves a large amount of computational time. The results of the calculations are given in Table 6. The order of accuracy of the prediction of emission is B3LYP < PBE0 < M06 < CAM-B3LYP < HF. The absolute deviation for B3LYP functional was found 0.06 to 0.18 eV. The PBE0 and M06 functionals predict the values with deviation of 0.17 to 0.30 eV. The CAM-B3LYP functional being intermediately accurate with deviation in the range of 0.40 to 0.56 eV, whereas HF method was found to be least accurate with deviations of 0.80 to 1.22 eV. The emission calculations with various functionals highlight the utility of the B3LYP functional to compute the emission energies of such kind of molecules. In the literature, the B3LYP functional has been successfully employed for estimating the vertical excitations of coumarin dye molecules [77, 78].

Conclusions

The optimized geometry for all the three molecules reveals that the donor group (N,N-diethylamino) is in-plane with the chromophoric system and helps in introducing a better conjugation in the system. The FMOs shows utility of presence of –CN group and non-participation of sulphonyl benzoic acid group in the photophysical behaviour of the molecule.

A careful analysis of the data computed with the chosen functionals and basis set reveals that the B3LYP functional predicts the lowest molecular energies in the gas phase as well

Table 6 Observed and calculated emission energies for **RC1, RC2** and **RC3** in various solvents (in eV)

	Observed	B3LYP		PBE0		M06		CAM-B3LYP		HF	
		Calc.	Diff.	Calc.	Diff.	Calc.	Diff.	Calc.	Diff.	Calc.	Diff.
RC1-CH_3CN	1.83	1.99	−0.16	2.06	−0.22	2.05	−0.22	2.24	−0.40	2.71	−0.88
RC1-DMSO	1.80	1.97	−0.17	2.04	−0.24	2.03	−0.23	2.22	−0.42	2.70	−0.89
RC1-$CHCl_3$	1.88	1.99	−0.11	2.06	−0.18	2.05	−0.17	2.23	−0.36	2.68	−0.80
RC2-CH_3CN	2.06	2.24	−0.18	2.35	−0.29	2.36	−0.30	2.62	−0.56	3.29	−1.23
RC2-DMSO	2.04	2.23	−0.18	2.34	−0.30	2.35	−0.30	2.60	−0.56	3.27	−1.22
RC3-CH_3CN	1.76	1.82	−0.06	1.99	−0.23	1.97	−0.21	2.17	−0.40	2.85	−1.09
RC3-DMSO	1.73	1.81	−0.08	1.99	−0.25	1.97	−0.24	2.15	−0.42	2.85	−1.12

as in the solution phase. The order of lower energy prediction is B3LYP < CAM-B3LYP < M06 < PBE0 < HF, where the HF method predicts highest energy value. The molecular energies calculated using triple zeta (6–311) basis set are lower than when calculated with double zeta 6–31 basis sets. This indicates the improvement of the results when triple zeta (6–311) basis set is used over double zeta (6–31) basis set.

But when it comes to the computations of the vertical excitation energies the trend is B3LYP < PBE0 < M06 < CAM-B3LYP < HF. The absolute deviation for the B3LYP functional was found ~0.20 eV and is the most suitable functional to compute vertical excitation energies of these kind of molecules. The basis sets reveal that the adding the polarization function to the basis set improved the computations of vertical excitations but diffused functions did not improve the results. The statistical treatment to the data proves that the B3LYP functional is most suitable for computing vertical excitations and emission calculation.

Acknowledgments Abhinav Tathe is thankful to University Grants Comission, New Delhi (India) for fellowship. LR and PR would like to acknowledge the facilities from the University of Mauritius

References

1. Chen C-T (2004) Evolution of red organic light-emitting diodes: materials and devices. Chem Mater 16:4389–4400. doi:10.1021/cm049679m
2. Yao Y-S, Zhou Q-X, Wang X-S et al (2007) A DCM-type red-fluorescent dopant for high-performance organic electroluminescent devices. Adv Funct Mater 17:93–100. doi:10.1002/adfm.200600055
3. Wu C, Tao S, Chen M et al (2013) A new multifunctional fluorenyl carbazole hybrid for high performance deep blue fluorescence, orange phosphorescent host and fluorescence/phosphorescence white OLEDs. Dyes Pigm 97:273–277. doi:10.1016/j.dyepig.2012.12.028
4. Zhang XH, Chen BJ, Lin XQ et al (2001) A new family of red dopants based on chromene-containing compounds for organic electroluminescent devices. Chem Mater 13:1565–1569. doi:10.1021/cm0008664
5. Kotani M, Kikuta J, Klauschen F et al (2013) Systemic circulation and bone recruitment of osteoclast precursors tracked by using fluorescent imaging techniques. J Immunol 190:605–612. doi:10.4049/jimmunol.1201345
6. Tynan CJ, Clarke DT, Coles BC et al (2012) Multicolour single molecule imaging in cells with near infra-red dyes. PLoS One 7:362–365. doi:10.1371/journal.pone.0036265
7. Kolmakov K, Belov VN, Wurm CA et al (2010) A versatile route to red-emitting carbopyronine dyes for optical microscopy and nanoscopy. European J Org Chem 3593–3610. doi: 10.1002/ejoc.201000343
8. Mitronova GY, Belov VN, Bossi ML et al (2010) New fluorinated rhodamines for optical microscopy and nanoscopy. Chemistry 16:4477–4488. doi:10.1002/chem.200903272
9. Sun Q, Li D, Dong G et al (2013) Improved organic optocouplers based on a deep blue fluorescent OLED and an optimized bilayer heterojunction photosensor. Sensors Actuators B Chem 188:879–885
10. Kessler F, Watanabe Y, Sasabe H et al (2013) High-performance pure blue phosphorescent OLED using a novel bis-heteroleptic iridium(iii) complex with fluorinated bipyridyl ligands. J Mater Chem C 1:1070. doi:10.1039/c2tc00836j
11. Kim S-J, Zhang Y, Zuniga C et al (2011) Efficient green OLED devices with an emissive layer comprised of phosphor-doped carbazole/bis-oxadiazole side-chain polymer blends. Org Electron 12:492–496
12. Ni YR, Su HQ, Huang W et al (2013) A spiro [fluorene-9, 9′-xanthene]-based host material for efficient green and blue phosphorescent OLED. Appl Mech Mater 331:503–507
13. Niesner R, Peker B, Schlüsche P, Gericke K-H (2004) Noniterative biexponential fluorescence lifetime imaging in the investigation of cellular metabolism by means of NAD(P)H autofluorescence. ChemPhysChem 5:1141–1149. doi:10.1002/cphc.200400066
14. Monici M (2005) Cell and tissue autofluorescence research and diagnostic applications. Biotechnol Annu Rev 11:227–256
15. Rich RM, Stankowska DL, Maliwal BP et al (2013) Elimination of autofluorescence background from fluorescence tissue images by use of time-gated detection and the AzaDiOxaTriAngulenium (ADOTA) fluorophore. Anal Bioanal Chem 405:2065–2075. doi:10.1007/s00216-012-6623-1
16. Behnke T, Mathejczyk JE, Brehm R et al (2013) Target-specific nanoparticles containing a broad band emissive NIR dye for the sensitive detection and characterization of tumor development. Biomaterials 34:160–170
17. Hong G, Lee JC, Robinson JT et al (2012) Multifunctional in vivo vascular imaging using near-infrared II fluorescence. Nat Med 18:1841–1846. doi:10.1038/nm.2995
18. Imasaka T, Tsukamoto A, Ishibashi N (1989) Visible semiconductor laser fluorometry. Anal Chem 61:2285–2288. doi:10.1021/ac00195a014
19. Shao F, Weissleder R, Hilderbrand SA (2008) Monofunctional carbocyanine dyes for bio- and bioorthogonal conjugation. Bioconjug Chem 19:2487–2491. doi:10.1021/bc800417b
20. Bouteiller C, Clavé G, Bernardin A et al (2007) Novel water-soluble near-infrared cyanine dyes: synthesis, spectral properties, and use in the preparation of internally quenched fluorescent probes. Bioconjug Chem 18:1303–1317. doi:10.1021/bc0700281
21. Lee H, Mason JC, Achilefu S (2006) Heptamethine cyanine dyes with a robust C-C bond at the central position of the chromophore. J Org Chem 71:7862–7865. doi:10.1021/jo061284u
22. Ying L-Q, Branchaud BP (2011) Facile synthesis of symmetric, monofunctional cyanine dyes for imaging applications. Bioconjug Chem 22:865–869. doi:10.1021/bc2001006
23. Mujumdar SR, Mujumdar RB, Grant CM, Waggoner AS (1996) Cyanine-labeling reagents: sulfobenzindocyanine succinimidyl esters. Bioconjug Chem 7:356–362. doi:10.1021/bc960021b
24. Romieu A, Tavernier-Lohr D, Pellet-Rostaing S et al (2010) Water solubilization of xanthene dyes by post-synthetic sulfonation in organic media. Tetrahedron Lett 51:3304–3308. doi:10.1016/j.tetlet.2010.04.080
25. Boyarskiy VP, Belov VN, Medda R et al (2008) Photostable, amino reactive and water-soluble fluorescent labels based on sulfonated rhodamine with a rigidized xanthene fragment. Chemistry 14:1784–1792. doi:10.1002/chem.200701058
26. Kolmakov K, Belov VN, Bierwagen J et al (2010) Red-emitting rhodamine dyes for fluorescence microscopy and nanoscopy. Chemistry 16:158–166. doi:10.1002/chem.200902309
27. Chen J, Liu W, Zhou B et al (2013) Coumarin- and rhodamine-fused deep red fluorescent dyes: synthesis, photophysical properties, and bioimaging in vitro. J Org Chem 78:6121–6130. doi:10.1021/jo400783x
28. Niu S, Massif C, Ulrich G et al (2012) Water-soluble red-emitting distyryl-borondipyrromethene (BODIPY) dyes for biolabeling. Chemistry 18:7229–72242. doi:10.1002/chem.201103613

29. Kajiwara Y, Nagai A, Chujo Y (2011) Red/near-infrared light-emitting organic-inorganic hybrids doped with covalently bound boron dipyrromethene (BODIPY) dyes via microwave-assisted one-pot process. Bull Chem Soc Jpn 84:471–481
30. Ortiz MJ, Garcia-Moreno I, Agarrabeitia AR et al (2010) Red-edge-wavelength finely-tunable laser action from new BODIPY dyes. Phys Chem Chem Phys 12:7804–7811. doi:10.1039/b925561c
31. Wang H, Li Z, Jiang Z et al (2005) Synthesis and properties of new orange red light-emitting hyperbranched and linear polymers derived from 3,5-dicyano-2,4,6-tristyrylpyridine. J Polym Sci A Polym Chem 43:493–504. doi:10.1002/pola.20511
32. Ishow E, Guillot R, Buntinx G, Poizat O (2012) Photoinduced intramolecular charge-transfer dynamics of a red-emitting dicyanovinyl-based triarylamine dye in solution. J Photochem Photobiol A Chem 234:27–36. doi:10.1016/j.jphotochem.2011.12.018
33. Chang YJ, Chow TJ (2011) Highly efficient red fluorescent dyes for organic light-emitting diodes. J Mater Chem 21:3091–3099. doi:10.1039/c0jm03109g
34. Sotgiu G, Galeotti M, Samorí C et al (2011) Push-pull amino succinimidyl ester thiophene-based fluorescent dyes: synthesis and optical characterization. Chemistry 17:7947–7952. doi:10.1002/chem.201100142
35. Alexander VM, Sano K, Yu Z et al (2012) Galactosyl human serum albumin-NMP1 conjugate: a near infrared (NIR)-activatable fluorescence imaging agent to detect peritoneal ovarian cancer metastases. Bioconjug Chem 23:1671–1679. doi:10.1021/bc3002419
36. Richard J-AJ-A, Massonneau M, Renard P-YP-Y, Romieu A (2008) 7-Hydroxycoumarin-hemicyanine hybrids: a new class of far-red emitting fluorogenic dyes. Org Lett 10:4175–4178. doi:10.1021/ol801582w
37. Kolmakov K, Wurm CA, Meineke DNH et al (2014) Polar red-emitting rhodamine dyes with reactive groups: synthesis, photophysical properties, and two-color STED nanoscopy applications. Chemistry 20:146–157. doi:10.1002/chem.201303433
38. Kolmakov K, Wurm C, Sednev MV et al (2012) Masked red-emitting carbopyronine dyes with photosensitive 2-diazo-1-indanone caging group. Photochem Photobiol Sci 11:522–532. doi:10.1039/c1pp05321c
39. Chen J, Liu W, Ma J et al (2012) Synthesis and properties of fluorescence dyes: tetracyclic pyrazolo[3,4-b]pyridine-based coumarin chromophores with intramolecular charge transfer character. J Org Chem 77:3475–3482. doi:10.1021/jo3002722
40. Krzeszewski M, Vakuliuk O, Gryko DT (2013) Color-tunable fluorescent dyes based on benzo[c]coumarin. Eur J Org Chem 2013:5631–5644. doi:10.1002/ejoc.201300374
41. Pashkova A, Chen H-S, Rejtar T et al (2005) Coumarin tags for analysis of peptides by MALDI-TOF MS and MS/MS. 2. Alexa Fluor 350 tag for increased peptide and protein identification by LC-MALDI-TOF/TOF MS. Anal Chem 77:2085–2096. doi:10.1021/ac048375g
42. Signore G, Nifosì R, Albertazzi L et al (2010) Polarity-sensitive coumarins tailored to live cell imaging. J Am Chem Soc 132:1276–1288. doi:10.1021/ja9050444
43. Cigáň M, Donovalová J, Szöcs V et al (2013) 7-(Dimethylamino)coumarin-3-carbaldehyde and its phenylsemicarbazone: TICT excited state modulation, fluorescent H-aggregates, and preferential solvation. J Phys Chem A 117:4870–4883. doi:10.1021/jp402627a
44. Moeckli P (1980) Preparation of some new red fluorescent 4-cyanocoumarin dyes. Dye Pigm 1:3–15
45. Huang S-T, Jian J-L, Peng H-Z et al (2010) The synthesis and optical characterization of novel iminocoumarin derivatives. Dye Pigm 86:6–14
46. Padilha L, Webster S, Przhonska OV et al (2010) Efficient two-photon absorbing acceptor-pi-acceptor polymethine dyes. J Phys Chem A 114:6493–6501. doi:10.1021/jp100963e
47. Wolfgang M, Dietmar A, Scheuermann H (1974) Farbstoffe der Benzopyranreihe. 1–28
48. Endo K, Murata Y (2000) Coumarin-based compound and its production. 1–6
49. Fujikawa H, Ishida N, Ohwaki T et al. (2002) Derive de coumarine, procede de production correspondant, agent et element luminescents contenant ledit derive. 1–15
50. Horst S, Dietmar A, Wolfgang M (1973) N-substituted imino-coumarin dyes. 1–16
51. Moeckli P (1985) Substituted Benzopyran compounds. 1–10
52. Moeckli P (1985) 2-(Oxo, or thio)-3-substituted 1,3-benzothiazolyl-4-cyano-7-substituted amino-benzopyrans. 1–10
53. Cave RJ, Burke K, Castner EW (2002) Theoretical investigation of the ground and excited states of Coumarin 151 and Coumarin 120. J Phys Chem A 106:9294–9305. doi:10.1021/jp026071x
54. Preat J, Loos P (2007) DFT and TD-DFT investigation of IR and UV spectra of solvated molecules: comparison of two SCRF continuum models. Int J Quantum Chem 107:574–585. doi:10.1002/qua
55. Cave RJ, Castner EW (2002) Time-dependent density functional theory investigation of the ground and excited states. J Phys Chem A 106:12117–12123
56. Tomasi J, Mennucci B, Cammi R (2005) Quantum mechanical continuum solvation models. Chem Rev 105:2999–3093. doi:10.1021/cr9904009
57. Wong MW, Frisch MJ, Wiberg KB (1991) Solvent effects. 1. The mediation of electrostatic effects by solvents. J Am Chem Soc 113:4776–4782. doi:10.1021/ja00013a010
58. Menzel R, Ogermann D, Kupfer S et al (2012) 4-Methoxy-1,3-thiazole based donor-acceptor dyes: characterization, X-ray structure, DFT calculations and test as sensitizers for DSSC. Dye Pigm 94:512–524. doi:10.1016/j.dyepig.2012.02.014
59. Kus N, Breda S, Reva I et al (2007) FTIR spectroscopic and theoretical study of the photochemistry of matrix-isolated coumarin. Photochem Photobiol 83:1237–1253
60. Seth D, Sarkar S, Sarkar N (2008) Solvent and rotational relaxation of coumarin 153 in a protic ionic liquid dimethylethanolammonium formate. J Phys Chem B 112:2629–2636. doi:10.1021/jp077416k
61. Spezia R, Zazza C, Palma A et al (2004) A DFT study of the low-lying singlet excited states of the all-trans peridinin in vacuo. J Phys Chem A 108:6763–6770. doi:10.1021/jp0496349
62. Bourbon P, Peng Q, Ferraudi G et al (2012) Synthesis, photophysical, photochemical, and computational studies of coumarin-labeled nicotinamide derivatives. J Org Chem 77:2756–2762. doi:10.1021/jo2025527
63. Satpati A, Senthilkumar S, Kumbhakar M et al (2005) Investigations of the solvent polarity effect on the photophysical properties of coumarin-7 dye. Photochem Photobiol 81:270–278
64. Xie L, Chen Y, Wu W et al (2012) Fluorescent coumarin derivatives with large stokes shift, dual emission and solid state luminescent properties: an experimental and theoretical study. Dye Pigm 92:1361–1369. doi:10.1016/j.dyepig.2011.09.023
65. Kohn W, Sham LJ (1965) Self-consistent equations including exchange and correlation effects. Phys Rev 140:A1133–A1138. doi:10.1103/PhysRev.140.A1133
66. Runge E, Gross EKU (1984) Density-functional theory for time-dependent systems. Phys Rev Lett 52:997–1000. doi:10.1103/PhysRevLett.52.997
67. Becke AD (1993) Density-functional thermochemistry. III. The role of exact exchange. J Chem Phys 98:5648. doi:10.1063/1.464913
68. Lee C, Yang W, Parr RG (1988) Development of the Colle-Salvetti correlation-energy formula into a functional of the electron density. Phys Rev B 37:785–789. doi:10.1103/PhysRevB.37.785

69. Yanai T, Tew DP, Handy NC (2004) A new hybrid exchange–correlation functional using the Coulomb-attenuating method (CAM-B3LYP). Chem Phys Lett 393:51–57. doi:10.1016/j.cplett.2004.06.011
70. Adamo C, Barone V (1999) Toward reliable density functional methods without adjustable parameters: the PBE0 model. J Chem Phys 110:6158. doi:10.1063/1.478522
71. Zhao Y, Truhlar DG (2007) The M06 suite of density functionals for main group thermochemistry, thermochemical kinetics, noncovalent interactions, excited states, and transition elements: two new functionals and systematic testing of four M06-class functionals and 12 other function. Theor Chem Acc 120:215–241. doi:10.1007/s00214-007-0310-x
72. Ditchfield R (1971) Self-consistent molecular-orbital methods. IX. An extended gaussian-type basis for molecular-orbital studies of organic molecules. J Chem Phys 54:724. doi:10.1063/1.1674902
73. Krishnan R, Schlegel HB, Pople JA (1980) Derivative studies in configuration–interaction theory. J Chem Phys 72:4654. doi:10.1063/1.439708
74. Frisch MJ, Trucks GW, Schlegel HB, Scuseria GE, Robb MA, Cheeseman JR, Scalmani G, Barone V, Mennucci B, Petersson GA, Nakatsuji H, Caricato M, Li X, Hratchian HP, Izmaylov AF, Bloino J, Zheng G, Sonnenberg JL, Hada M, Ehara M, Toyota K, Fukuda R, Hasegaw CJ (2010) Fox DJ (2010) Gaussian 09 revision C01
75. Dooley R, Milfeld K, Guiang C et al (2006) From proposal to production: lessons learned developing the computational chemistry grid cyberinfrastructure. J Grid Comput 4:195–208
76. Shen N, Fan Y, Pamidighantam S (2014) E-science infrastructures for molecular modeling and parametrization. J Comput Sci 5:576–589. doi:10.1016/j.jocs.2014.01.005
77. Sakata T, Kawashima Y, Nakano H (2009) Low-lying excited states of 7-aminocoumarin derivatives: a theoretical study. Int J Quantum Chem 109:1940–1949. doi:10.1002/qua.22019
78. Georgieva I, Trendafilova N, Aquino A, Lischka H (2005) Excited state properties of 7-Hydroxy-4-methylcoumarin in the gas phase and in solution. A theoretical study. J Phys Chem A 109:11860–11869. doi:10.1021/jp0524025